February 2000 • NREL/CP-520-27699

Conference Paper

CuPt-B Ordered Microstructures in GaInP and GaInAs Films

S.P. Ahrenkiel, K.M. Jones, R.J. Matson, M.M. Al-Jassim, Y. Zhang, A. Mascarenhas, D.J. Friedman, D.J. Arent, J.M. Olson, and M.C. Hanna

Presented at the Materials Research Society's 1999 Fall Meeting
Boston, Massachusetts
November 29 – December 3, 1999

National Renewable Energy Laboratory

1617 Cole Boulevard
Golden, Colorado 80401-3393

NREL is a U.S. Department of Energy Laboratory
Operated by Midwest Research Institute • Battelle • Bechtel

Contract No. DE-AC36-99-GO10337

CuPt-B ORDERED MICROSTRUCTURES IN GaInP AND GaInAs FILMS

S. P. AHRENKIEL, K. M. JONES, R. J. MATSON, M. M. AL-JASSIM,
Y. ZHANG, A. MASCARENHAS,
D. J. FRIEDMAN, D. J. ARENT, J. M. OLSON, M. C. HANNA
National Renewable Energy Laboratory, Golden, Colorado 80401

ABSTRACT

We examine CuPt-B atomic sublattice ordering in $Ga_{0.51}In_{0.49}P$ (GaInP) and $Ga_{0.47}In_{0.53}As$ (GaInAs) III-V alloy films grown by atmospheric- and low-pressure metalorganic chemical vapor deposition on singular and vicinal (001) substrates. The influences of growth conditions and substrate miscut on double- and single-variant ordered microstructures are investigated using transmission electron microscopy (TEM). Relatively thick (>1-2 μm) double-variant ordered GaInP and GaInAs films show complementary superdomain formation. Single-variant ordered films on <111>B-miscut substrates contain single-phase domains, separated by antiphase boundaries (APBs). The appearance of APBs in TEM dark-field images is anticipated from electron diffraction theory.

INTRODUCTION

CuPt-B atomic ordering occurs in several epitaxial III-V alloys grown under appropriate conditions. $Ga_{0.51}In_{0.49}P$ (GaInP) on GaAs and $Ga_{0.47}In_{0.53}As$ (GaInAs) on InP are prominent examples. The influences of ordering on the optoelectronic properties of these materials, such as reduced bandgap energy [1,2], birefringence [3], anisotropic carrier mobilities [4], and extended carrier lifetimes [5], have been considered for device applications.

Several groups have proposed kinetic origins for CuPt-B ordering in III-Vs [6,7]. Growth models are guided by *in situ* surface analyses. Metal-organic chemical vapor deposition (MOCVD) generates strong CuPt-B ordering, while also providing good film uniformity and throughput. The low pressures and fluxes used in molecular beam epitaxy (MBE) accommodate additional analyses by electron-diffraction techniques. (2×) reconstructions have been associated with CuPt-B ordering in both MOCVD and MBE [8]. Synthetic CuPt-B ordering has also been generated by MBE of GaP/InP short-period superlattices on {111}B substrates [9].

In this proceeding, we present combined microstructural results from several sets of CuPt-B ordered GaInP and GaInAs films grown in various MOCVD systems at NREL.

EXPERIMENT

MOCVD

GaInP films were grown by atmospheric-pressure MOCVD using trimethylgallium, trimethylindium, and phosphine sources at 640°C-680°C, 5.5 μm/hr, with a V/III flux ratio of 58.7. Growth was conducted on up to four substrates (with various orientations) in a single run.

GaInAs films were grown by low-pressure MOCVD from trimethylgallium, trimethylindium, and arsine sources at 500°C-600°C, 1.4 Å/s-9.5 Å/s, with total thicknesses up to 1.5 μm. Both hydrogen and nitrogen were used as group-V carrier gases.

TEM

Cross sections were cleaved near <110> faces, then thinned and glued to Si blocks, polished, dimpled, and milled at low angle with 3.5-4-kV Ar^+ ions for 2-5 h using $L\text{-}N_2$ cooling. For plan view, films were glued to Cu grids with silver paste, then thinned, dimpled, and milled from the substrate side to perforation.

Selected-area electron diffraction patterns (DPs), dark-field (DF) images, and lattice images were acquired on a CM30 TEM with a 12-bit charge-coupled device camera operated at 300 kV. In cross section, samples were oriented near <110>A, or a <310>, located 26.6° about [001] from <110>B. Plan-view examinations were performed near <114>A (19.5° from [001]).

A mixture C of DF images A and B from complementary ordered domains

$$C = (1-\eta)|A+B| + \eta|A-B| \qquad (1)$$

shows enhanced similarities with mixing parameter $\eta = 0$, and enhanced differences with $\eta = 1$.

Image FFTs are linear mixtures of original image FFTs $I(\mathbf{g})$ with filtered copies $O(\mathbf{g})I(\mathbf{g})$. The filter functions $O(\mathbf{g})$ are judiciously selected sums of eccentric Gaussian masks, which are often Fresnel pairs. The filtered image is generated by inverse transformation of the filtered FFT

$$I'(\mathbf{g}) = [(1-f) + fO(\mathbf{g})]I(\mathbf{g}) \qquad (2)$$

The filtering parameter $0 \leq f \leq 1$ varies the emphasis of periodic features in lattice images.

RESULTS

The relative ordering strength and domain geometry of each CuPt-B variant are strongly influenced by small substrate miscuts from [001] in both GaInP and GaInAs. In addition, domain evolution in double-variant films is often coupled to nonplanar surface topography, generating additional microstructural inhomogeneity with continued growth. Single-variant films are less subject to evolution, but often show an increase in the mean size of single-phase domains during growth. We discuss the appearance of the associated APBs in TEM DF images.

GaInP

Ordered GaInP microstructural details were reported by Baxter et al. [10]. Symmetric double-variant ordering occurs on 0° GaAs. On 2°AB GaAs, the double-variant ordering is asymmetric. Single-variant ordering occurs at 4°B [Fig. 1]. The diffraction spots are often broadened by small domain sizes and inhomogeneity in the ordered microstructure.

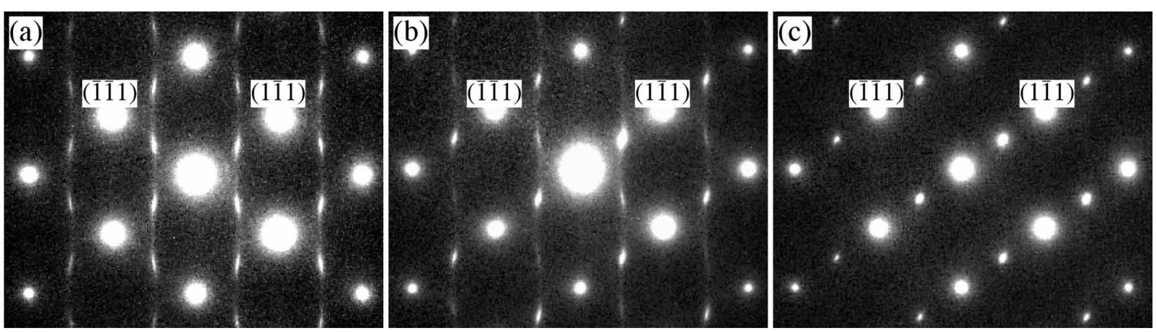

Fig. 1. Near-interface DPs of GaInP on (a) 0°, (b) 2°AB, and (c) 4°B GaAs.

The near-interface double-variant structure on 0° GaAs comprises vertically stacked lamellae alternating between variants on a length scale of 40-50 Å, and sectioned by APBs. Beyond a few μm thickness, the variants form laterally segregated superdomains on a length scale near the film thickness [11]. Both variants typically contain numerous APBs that section the single-variant domains into numerous single-phase regions [Fig. 2]. The APB geometry is dictated by the local variant and surface orientation.

Double-variant GaInP on 0° GaAs typically shows irregular surfaces [Fig. 3], corresponding to a broad distribution of domain sizes.

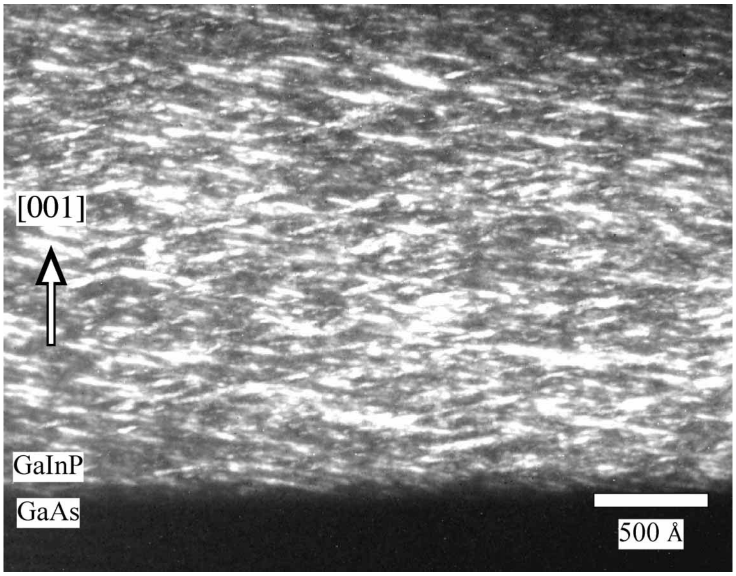

Fig. 2. Mixed near-interface DF image of GaInP on 0° GaAs.

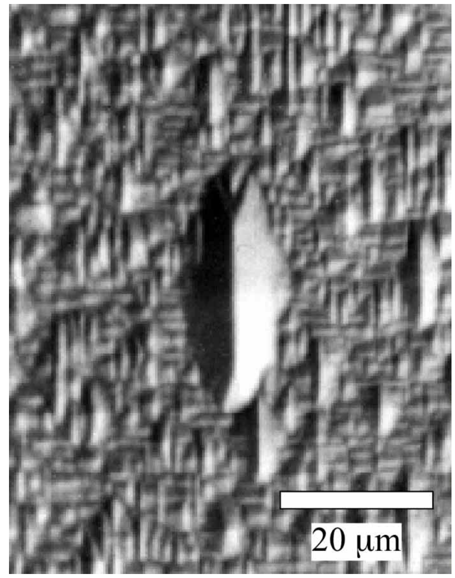

Fig. 3. Optical image of GaInP surface on 0° GaAs.

Variant segregation is enhanced in GaInP on 2°AB GaAs. Superdomain formation is evident below 0.5-μm thickness. The surface develops asymmetric facets [Fig. 4] correlated to the underlying superdomain structure [Fig. 5]. The reduced competition between the variants results in improved regularity of the surface topography, and a relatively narrow distribution of facet sizes compared to GaInP on 0° GaAs.

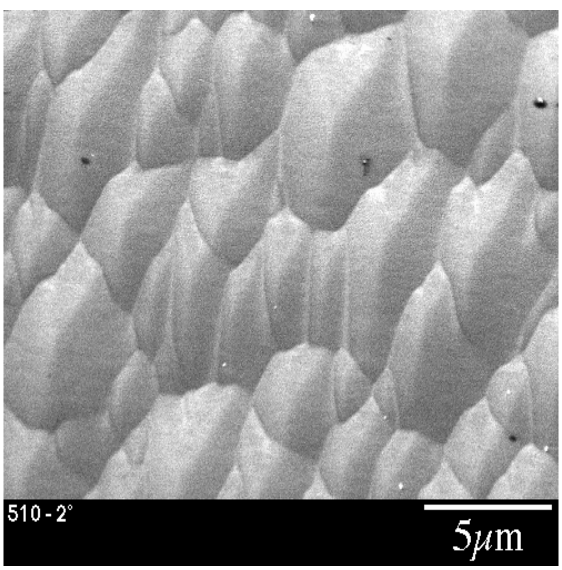

Fig. 4. SEM image of 6-μm-thick GaInP surface on 2°AB GaAs.

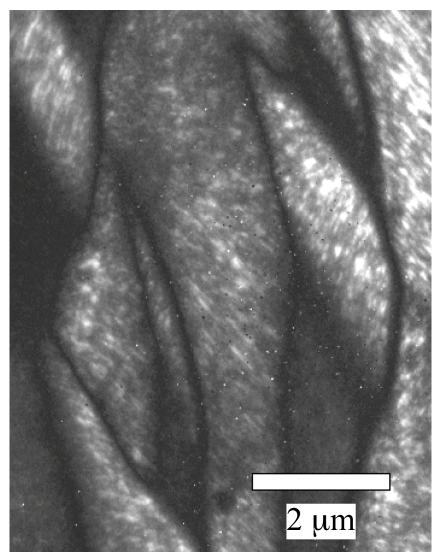

Fig. 5. Mixed plan-view DF image of GaInP on 2°AB GaAs.

The strength of ordering, the rate of variant segregation, and the mean vertical dimension of near-interface ordered lamellae decrease with <111>A miscut. The near-interface microstructures at 2°A and 6°A are qualitatively similar to that at 0°. At 2°A, complementary superdomains emerge near 3-μm thickness [Fig. 6]. At 6°A, we observe only weak variant segregation beyond 5-μm thickness, with diffuse superdomains and a rippled topography. Vertical, nonperiodic order/disorder stacking is observed within the superdomains on a length scale of 200 Å [Fig. 7]. The ordered lamina extend across superdomain boundaries, with an abrupt change in local variant. The vertical variations in ordering strength may be coupled to small composition fluctuations that arise from nonuniform source vapor fluxes during growth.

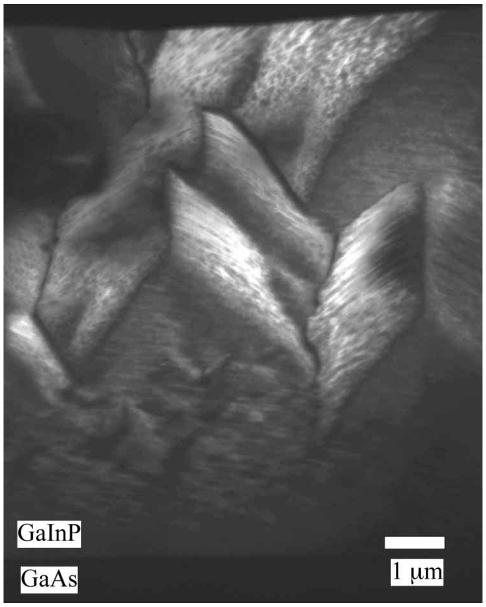

Fig. 6. Mixed DF image of GaInP on 2°A GaAs.

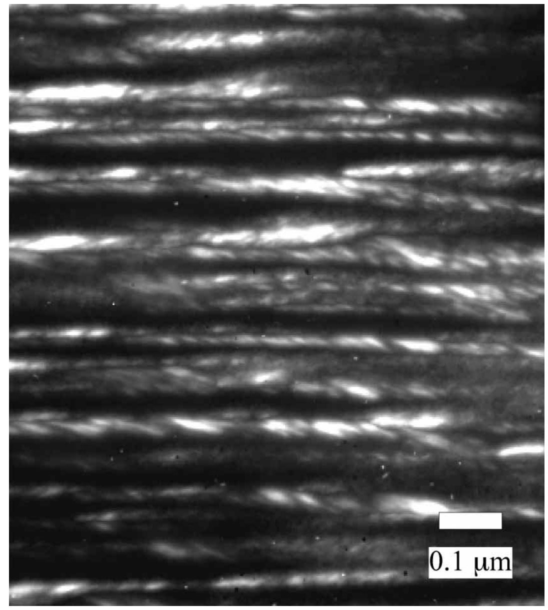

Fig. 7. Mixed DF image of GaInP on 6°A GaAs.

Variant segregation is completely suppressed to 10-µm thickness in 15.8°A samples grown under typical conditions. The DPs are similar to those from low-temperature samples, which show intensity minima near the locations of the ordered spots [11]. This ordering comprises weakly ordered lamellae aligned on alternating (002) MLs, with a coherence length of only a few MLs, whereas alternating (002) MLs are anticorrelated in the CuPt-B structure.

Single-variant GaInP generally contains APBs (o/o') with their normals inclined from [001] towards the ordering direction [Fig. 8].

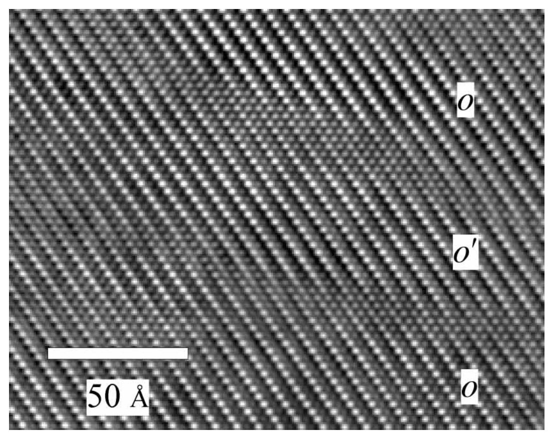

Fig. 8. Filtered <110>A lattice image of GaInP on 2°B GaAs.

GaInAs

A detailed study of ordered GaInAs microstructures on 0° substrates was conducted by Seong et al. [12]. We have varied growth parameters near the optimal conditions for ordering in GaInAs on InP substrates miscut 0°, 2°AB, and 6°B. We find improved surface topographies using hydrogen as the group-V carrier gas, rather than nitrogen. Increased temperature [Fig. 9]

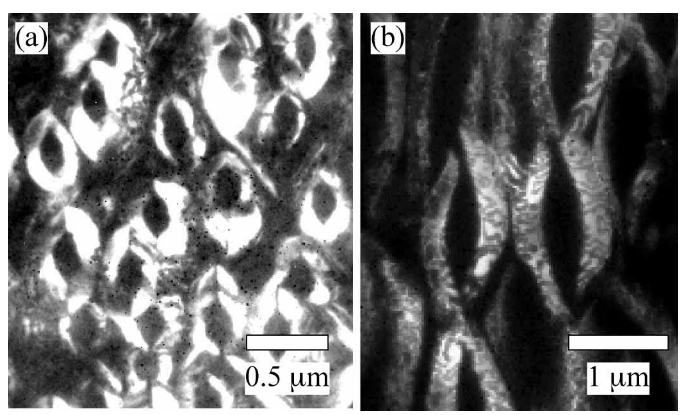

Fig. 9. GaInAs on 0° InP at (a) 525°C, (b) 575°C.

and reduced rate [Fig. 10] have similar influences on the resulting ordered microstructures in GaInAs. (The growth rate was controlled by varying the V/III ratio with constant group-V flux.) Both increase the mean domain sizes, and generate large, disordered regions. At high growth rates, the domains show sharp profiles, and tend to align along <110>B in the substrate plane.

APBs in single-variant GaInAs are often inclined in the opposite direction from the growth plane compared to GaInP. The origin of this tilt has been associated with surface diffusion rates and step densities [13]. APB inclinations have also been correlated to the presence of supersteps on the growth surface [14].

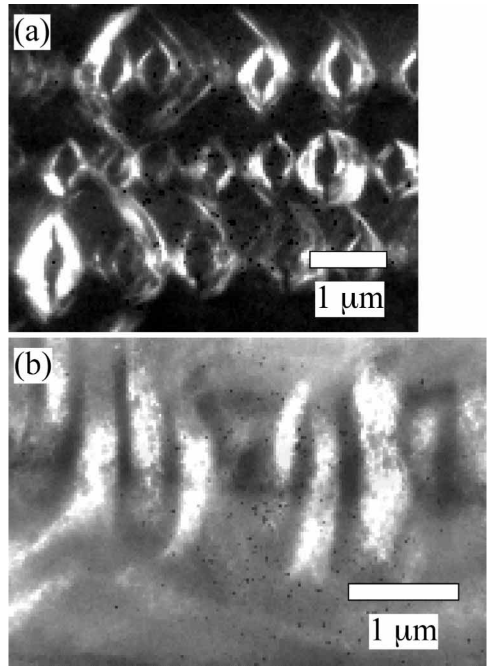

Fig. 10. GaInAs on 0° InP grown at (a) 9.5 Å/s, (b) 1.4 Å/s.

APB Dark-Field Contrast

APBs are a variety of stacking fault with a relative phase of 180°. We calculate the dynamically diffracted intensity below the surface of a thin foil of thickness T containing an APB at depth t $(0 < t < T)$. For simplicity, we retain only the direct beam 0 and a diffracted beam g.

Continuity of the electron wave function and its gradient are required at all interfaces. However, exact continuity of the gradient requires back-scattered waves, which we ignore. We assume the potential component $U_{\mathbf{g}}$ is a real quantity, without loss of generality, and identify the extinction distance $\xi = k/U_{\mathbf{g}}$, where k is the incident wave number. The beam amplitudes vary with excitation error s (the distance from g to the Ewald sphere surface, measured parallel to the foil normal). At the Bragg condition ($s = 0$), with $T = \xi/2$, the DF image intensity is

$$I_{DF} = \cos^2(\pi\, t/T) \qquad (3)$$

The diffracted intensity vanishes when $t/T = 0.5$, such that the APB appears darkest when it vertically separates equal thicknesses of phase and antiphase material. The depth of a planar APB inclined to the surface of the foil varies linearly in the range $0 \le t \le T$. Experimental APB contrast acquired in plan view from a 6°B sample at various tilts from the Bragg condition [Fig. 11] shows other identifiable forms that resemble calculated intensity profiles, assuming comparable excitation of the diffracted spot.

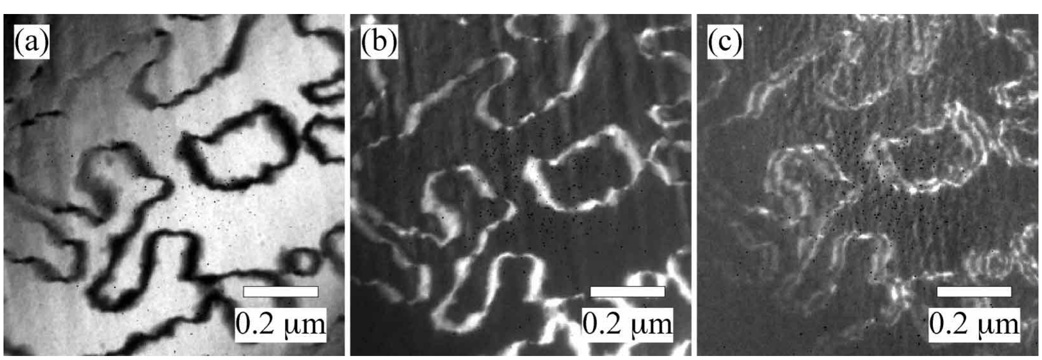

Fig. 11. GaInAs on 6°B InP tilted approximately (a) 0°, (b) 0.1°, and (c) 0.3° from the Bragg condition.

CONCLUSIONS

The influences of substrate miscut on ordered microstructures in GaInP and GaInAs films are qualitatively similar. However, the near-interface lamellar structure observed in GaInP on 0° GaAs has not been clearly identified in GaInAs. In GaInP, the inclination of the APBs from the substrate plane increases monotonically with miscut from 2°B to 6°B. However, we observe the opposite inclination of the APBs from the substrate plane in the available GaInAs samples. Diffraction analysis confirms that the physical nature of the APBs is identical in the two systems. Therefore, the observed differences may facilitate an improved understanding of the mechanism for the vertical propagation of APBs in these materials

ACKNOWLEDGMENTS

We are grateful to C. Kramer for technical assistance, and to S. Kurtz for providing comparative samples.

REFERENCES

1. A. Gomyo, T. Suzuki, K. Kobayashi. S. Kawata, I. Hino, and T. Yuasa, Appl. Phys. Letters 50 (1987) 673.

2. D. J. Arent, K. A. Bertness, M. Bode, Sarah R. Kurtz, and J. M. Olson, Appl. Phys. Letters 62 (1993) 1806.

3. F. Alsina, M. Garriga, M. I. Alonso, J. Pascual, J. Camassel, and R. W. Glew in 22nd International Conference on the Physics of Semiconductors, Ed. D. J. Lockwood, (World Scientific, Vancouver, Canada, 1994), pp. 253-256.

4. O. Ueda in Optoelectronic Materials: Ordering, Composition Modulation, and Self-Assembled Structures, Ed. E. D. Jones, A. Mascarenhas, P. Petroff, (Materials Research Society, Pittsburgh, Vol. 417, 1996), pp. 31-42.

5. S. P. Ahrenkiel, S. W. Johnston, R. K. Ahrenkiel, D. J. Arent, M. C. Hanna, and M. W. Wanlass, Appl. Phys. Letters 74 (1999) 3534.

6. S. Froyen and A. Zunger, Phys. Rev. Letters 66 (1991) 2132 .

7. T. Suzuki and A. Gomyo, J. Cryst. Growth 111 (1991) 353.

8. T. Suzuki, T. Ichihashi, and T. Nakayama, Appl. Phys. Letters 73 (1998) 2588.

9. S.-J. Kim, H. Asahi, M. Takemoto, K. Asami, M. Takeuchi, and S.-I. Gonda., Jpn. J. Appl. Phys. 33 (1996) 4225.

10. C. S. Baxter, W. M. Stobbs, and J. H. Wilkie, J. Crystal Growth, 112 (1991) 373.

11. D. J. Friedman, J. G. Zhu, A. E. Kibbler, J. M. Olson, and J. Moreland, Appl. Phys. Letters 63 (1993) 1774.

12. T. Y. Seong, A. G. Norman, G. R. Booker, and A. G. Cullis, J. Appl. Phys. 75 (1994) 12.

13. S. Takeda, Y. Kuno, N. Hosoi, and K. Shimoyama, J. Crystal Growth 205 (1999) 11.

14. S. H. Lee and G. B. Stringfellow, J. Appl. Phys. 83 (1998) 3620.

REPORT DOCUMENTATION PAGE

Form Approved
OMB NO. 0704-0188

1. AGENCY USE ONLY (Leave blank)	2. REPORT DATE February 2000	3. REPORT TYPE AND DATES COVERED conference paper	
4. TITLE AND SUBTITLE CuPt-B Ordered Microstructures in GaInP and GaInAs Films			5. FUNDING NUMBERS C TA: PV003201
6. AUTHOR(S) S.P. Ahrenkiel, K.M. Jones, R.J. Matson, M.M. Al-Jassim, Y. Zhang, A. Mascarenhas, D.J. Friedman, D.J. Arent, J.M. Olson, M.C. Hanna			
7. PERFORMING ORGANIZATION NAME(S) AND ADDRESS(ES)			8. PERFORMING ORGANIZATION REPORT NUMBER
9. SPONSORING/MONITORING AGENCY NAME(S) AND ADDRESS(ES) National Renewable Energy Laboratory 1617 Cole Blvd. Golden, CO 80401-3393			10. SPONSORING/MONITORING AGENCY REPORT NUMBER CP-520-27699
11. SUPPLEMENTARY NOTES			
12a. DISTRIBUTION/AVAILABILITY STATEMENT National Technical Information Service U.S. Department of Commerce 5285 Port Royal Road Springfield, VA 22161			12b. DISTRIBUTION CODE

13. ABSTRACT *(Maximum 200 words)*

We examine CuPt-B atomic sublattice ordering in $Ga_{0.51}In_{0.49}P$ (GaInP) and $Ga_{0.47}In_{0.53}As$ (GaInAs) III-V alloy films grown by atmospheric- and low-pressure metalorganic chemical vapor deposition on singular and vicinal (001) substrates. The influences of growth conditions and substrate miscut on double- and single-variant ordered microstructures are investigated using transmission electron microscopy (TEM). Relatively thick (>1-2 µm) double-variant ordered GaInP and GaInAs films show complementary superdomain formation. Single-variant ordered films on <111>B-miscut substrates contain single-phase domains, separated by antiphase boundaries (APBs). The appearance of APBs in TEM dark-field images is anticipated from electron diffraction theory.

14. SUBJECT TERMS photovoltaics ; GaInP ; GaInAs ; III-V alloy films ; metalorganic chemical vapor deposition ; transmission electron microscopy ; CuPt-B ordering ; microstructures ; miscuts			15. NUMBER OF PAGES 16. PRICE CODE
17. SECURITY CLASSIFICATION OF REPORT Unclassified	18. SECURITY CLASSIFICATION OF THIS PAGE Unclassified	19. SECURITY CLASSIFICATION OF ABSTRACT Unclassified	20. LIMITATION OF ABSTRACT UL